Smyth DJ, Cooper JD, Bailey R, Field S, Burren O, Smink LJ, Guja C, Ionescu-Tirgoviste C, Widmer B, Dunger DB, et al. 2006. A genome-wide association study of nonsynonymous SNPs identifies a type 1 diabetes locus in the interferon-induced helicase (IFIH1) region. *Nat Genet.* 38:617–619.

Stevison LS, Kohn MH. 2008. Determining genetic background in captive stocks of cynomolgus macaques (*Macaca fascicularis*). *J Med Primatol.* 37:311–317.

Stredrick DL, Garcia-Closas M, Pineda MA, Bhatti P, Alexander BH, Doody MM, Lissowska J, Peplonska B, Brinton LA, Chanock SJ, et al. 2006. The ATM missense mutation p.ser49cys (c.146C-G) and the risk of breast cancer. *Hum Mutat.* 27:538–544.

Suntharalingam G, Perry MR, Ward S, Brett SJ, Castello-Cortes A, Brunner MD, Panoskaltsis N. 2006. Cytokine storm in a phase 1 trial of the anti-CD28 monoclonal antibody TGN1412. *New Engl J Med.* 355:1018–1028.

Tosi AJ, Morales JC, Melnick DJ. 2002. Y-chromosome and mitochondrial markers in *Macaca fascicularis* indicate introgression with Indochinese *M. mulatta* and a biogeographic barrier in the Isthmus of Kra. *Int J Primatol.* 23:161–178.

Tosi AJ, Morales JC, Melnick DJ. 2003. Paternal, maternal, and biparental molecular markers provide unique windows onto the evolutionary history of macaque monkeys. *Evolution* 57: 1419–1435.

Wang S. 1998. China Red Data Book of Endangered Animal (Mammalia). Beijing: Science Press.

Yan G, Zhang G, Fang X, Zhang Y, Li C, Ling F, Cooper DN, Li Q, Li Y, van Gool AJ, et al. 2011. Genome sequencing and comparison of two nonhuman primate animal models, the cynomolgus and Chinese rhesus macaques. *Nat Biotechnol.* 29:1019–1023.

Yang F, Wang HX, Zhou L, Ai YX, Zeng T. 2010. A primary analyze and measurement on partial biochemistry index of peripheral blood cells of *Macaca thibetana*. *Sichuan J Zool.* 29:256–258.

Yao YF, Zhong LJ, Liu BF, Li JY, Ni QY, Xu HL. 2013. Genetic variation between two Tibetan macaque (*Macaca thibetana*) populations in the eastern China based on mitochondrial DNA control region sequences. *Mitochondr DNA.* 24:267–275.

Zhao QK. 1994. Mating competition and intergroup transfer of males in Tibetan macaques (*Macaca thibetana*) at Mt Emei, China. *Primates* 35:57–68.

Zheng BX, Xu QQ, Shen YP. 2002. The relationship between climate change and Quaternary glacial cycles on the Qinghai-Tibetan Plateau: review and speculation. *Quaternary Int.* 97–98: 93–101.

Zhong LJ, Zhang MW, Yao YF, Ni QY, Mu J, Li CQ, Xu HL. 2013. Genetic diversity of two Tibetan macaque (*Macaca thibetana*) populations from Guizhou and Yunnan in China based on mitochondrial DNA D-loop sequences. *Genes Genomics.* 35:205–214.

Ziegler T, Abegg C, Meijaard E, Perwitasari-Farajallah D, Walter L, Hodges JK, Roos C. 2007. Molecular phylogeny and evolutionary history of Southeast Asian macaques forming the *M. silenus* group. *Mol Phylogenet Evol.* 42:807–816.

Original Paper

nephron
Experimental
Nephrology

Nephron Exp Nephrol 2013;123:22–33
DOI: 10.1159/000354058

Received: February 21, 2013
Accepted: June 26, 2013
Published online: August 23, 2013

# Tenc1-Deficient Mice Develop Glomerular Disease in a Strain-Specific Manner

Kozue Uchio-Yamada[a] Kyoko Sawada[a] Kotaro Tamura[c] Sumie Katayama[b]
Youko Monobe[b] Yoshie Yamamoto[d] Atsuo Ogura[e] Noboru Manabe[f]

[a]Laboratory of Animal Models for Human Diseases, [b]Section of Laboratory Equipment, National Institute of Biomedical Innovation, Ibaraki, [c]Drug Safety Research Laboratories, Astellas Pharma Inc., Osaka, [d]Department of Veterinary Science, National Institute of Infectious Diseases, Tokyo, [e]RIKEN BioResouce Center, Tsukuba, and [f]Animal Resource Center, The University of Tokyo, Kasama, Japan

**Key Words**
Tenc1 (tensin2) · Nephrotic syndrome · ICR-derived glomerulonephritis mouse · Integrin · Glomerular basement membrane · Podocyte

**Abstract**
***Background/Aims:*** Tenc1 (also known as tensin2) is an integrin-associated focal adhesion molecule that is broadly expressed in mouse tissues including the liver, muscle, heart and kidney. A mouse strain carrying mutated *Tenc1*, the ICR-derived glomerulonephritis (ICGN) strain, develops severe nephrotic syndrome. ***Methods:*** To elucidate the function of Tenc1 in the kidney, *Tenc1*$^{ICGN}$ was introduced into 2 genetic backgrounds, i.e. DBA/2J (D2) and C57BL/6J (B6), strains that are respectively susceptible and resistant to chronic kidney disease. ***Results:*** Biochemical and histological analysis revealed that homozygous *Tenc1*$^{ICGN}$ mice develop nephrotic syndrome on the D2 background (D2GN) but not on the B6 background (B6GN). Initially, abnormal assembly and maturation of glomerular basement membrane (GBM) were observed, and subsequently effacement of podocyte foot processes was noted in the kidneys of D2GN but not B6GN mice. These defects are likely to be involved in the integrin signaling pathway. ***Conclusion:*** This study suggests that Tenc1 contributes to the maintenance of GBM structures and that the genetic background influences the severity of nephrotic syndrome.


## Introduction

Congenital nephrotic syndrome is characterized by massive proteinuria, hypoalbuminemia, edema and hyperlipidemia [1]. The cardinal feature of nephrotic syndrome is severe proteinuria resulting from an increased flux of albumin and other plasma proteins across the glomerular filtration barrier, which is composed of 3 layers, namely the fenestrated endothelium, glomerular basement membrane (GBM) and podocyte layer with foot processes and slit diaphragms [2–4]. It is known that proteinuria can be caused by a primary defect in the GBM and/or podocytes [3]. The GBM is a network formed by laminin, collagen IV, nidogen and negatively charged proteoglycans [4], and among the components, substitutions of laminin and collagen IV occur during glomerular maturation [5–7]. During the early stage of glomerular

KARGER

1660–2129/13/1234–0022$38.00/0

E-Mail karger@karger.com
www.karger.com/nee

Kozue Uchio-Yamada, PhD
Laboratory of Animal Models for Human Diseases
National Institute of Biomedical Innovation
7-6-8 Saito-Asagi, Ibaraki 567-0085 (Japan)
E-Mail kozue-mt@nibio.go.jp

development, laminin-1 (α1β1γ1) is synthesized but is finally removed and replaced by laminin-11 (α5β2γ1), which is the only laminin present in the mature GBM [5, 6]. A similar shift occurs in collagen IV; that is, the early GBM contains α1 and α2 chains *(COL4A1* and *COL4A2)*, but the mature GBM contains α3, α4 and α5 chains *(COL4A3, COL4A4* and *COL4A5)* [5, 6]. The defective expression of mature GBM isoforms causes abnormalities in the glomerular structure and function, namely Pierson's syndrome due to mutation of laminin β2 [7, 8] and Alport syndrome due to mutation of *COL4A3–COL4A5* [9]. Besides GBM disorganization, proteinuria is attributed to effacement of podocyte foot processes [2]. Nephrin and podocin are the major structural elements of the slit diaphragms connecting adjacent foot processes, and mutations of these genes are responsible for congenital nephrotic syndrome [10, 11]. Furthermore, alterations in α3β1 integrin, which anchors podocyte foot processes to the GBM, also give rise to GBM abnormalities and effacement of foot processes [12]. Integrin-linking kinase (ILK) and focal adhesion kinase (FAK), which are downstream regulators of integrin β1, are also related to the onset of glomerular diseases [13–16]. Key structural proteins in the glomerular filtration barrier have been identified, but the disease mechanisms of nephrotic syndrome remain unresolved.

The ICR-derived glomerulonephritis (ICGN) mouse is considered to be a good model of congenital nephrotic syndrome [17, 18]. The ICGN mouse possesses a mutated Tencl (also known as tensin2), comprising an 8-bp deletion (nucleotides 1477–1484) in exon 18, and this mutation causes a frameshift, leading to a terminal codon at nucleotide 1538 [18]. Tencl is expressed in podocytes and tubules in normal mouse kidneys but not in ICGN mice [18]. Tencl, a member of the tensin family, is an integrin-mediated focal adhesion molecule that regulates cell migration [19, 20]. Tencl possesses a protein kinase C (PKC)- and actin-binding domain at the N terminus, src homology 2 (SH2), and phosphotyrosine-binding (PTB) domains at the C terminus, and is widely distributed in mouse tissues including the heart, liver, kidney and skeletal muscle [19–22]. The function of Tencl in the kidney and its involvement in the development of nephrotic syndrome remain poorly understood [23, 24]. In the present study, to reveal the function of Tencl in the kidney, *Tencl*$^{ICGN}$ was introduced into 2 genetic backgrounds, namely DBA/2J (D2) and C57BL/6J (B6), strains that are respectively susceptible and resistant to chronic kidney disease. We investigated the phenotype of *Tencl*$^{ICGN}$ mice on the D2 background (D2GN) and B6 background (B6GN).

## Materials and Methods

*Animals*

Male ICGN mice maintained at the National Institute of Biomedical Innovation and D2 and B6 mice purchased from Clea Japan (Tokyo, Japan) were used in this study. All animals were housed in autoclaved cages in an air-conditioned room (23 ± 1°C) under controlled lighting conditions (12 h light/12 h dark) and were given a standard diet (CMF, Oriental Yeast, Tokyo, Japan) and tap water ad libitum. All animal experiments were performed in accordance with protocols approved by the Institutional Animal Care and Use Committee of the National Institute of Biomedical Innovation. The *Tencl* mutation of the ICGN strain was introduced into 2 genetic backgrounds, D2 and B6. Two congenic strains, D2GN and B6GN, were made by generating an F1 hybrid between ICGN and D2 or B6 followed by 12 generations of marker-assisted backcrossing to D2 or B6. The marker-assisted speed congenic method resulted in a >99% replacement of the D2 or B6 background genome by the N6 generation. N12 mice were then intercrossed to generate *Tencl*$^{ICGN}$ homozygous mice.

*Genotyping*

Genomic DNA was isolated from a short piece of tail. Genotyping was determined by PCR with Tencl gene-specific primers. The following primers were used: sense, 5′-CCCGATGCTCTCTGTCAGCA-3′, and antisense, 5′-CGATCCAGCTCCTGTCTTTC-3′. The 5′ end of the sense primer was labeled with Beckman Dye4 (Sigma, St. Louis, Mo., USA). PCR was performed using a Go Taq Green Master Mix (Promega, Madison, Wisc., USA) for 35 cycles of 94°C for 30 s, 60°C for 30 s and 72°C for 30 s, followed by a final extension at 72°C for 7 min. After amplification, samples were electrophoresed and analyzed by CEQ8800 (Beckman Coulter, Brea, Calif., USA).

*Measurements in Serum and Urine*

Mice were anesthetized with somnopentyl (Kyoritsu Seiyaku, Tokyo, Japan), and blood was collected by cardiac puncture. Serum albumin, creatinine, blood urea nitrogen and total cholesterol levels were measured on an automatic analyzer (Fuji Dri-Chem FDC7000, Fujifilm, Tokyo, Japan). Urine was collected from 2-, 4-, 10-, 20- and 40-week-old mice, and urine albumin levels were analyzed by SDS-PAGE, followed by Coomassie Brilliant Blue staining.

*Glomerular Isolation*

Glomerular isolation was performed according to the methods described by Takemoto et al. [25]. Briefly, male 8-, 10- and 20-week-old D2 mice and D2GN mice were anesthetized by intraperitoneal injection of somnopentyl and perfused with $8 \times 10^7$ M-450 dynabeads (Invitrogen, Carlsbad, Calif., USA) diluted in 40 ml of Hanks' balanced salt solution through their heart. After perfusion, the kidneys were removed, cut into small pieces (1 $mm^3$) and digested in collagenase A (1 mg/ml) and DNase I (100 IU/ml) at 37°C for 30 min with gentle shaking. After digestion, the tissues were gently pressed through a 100-μm cell strainer. Glomeruli that contained Dynabeads were then gathered using a magnetic particle concentrator. Isolated glomeruli were washed 3 times with cold Hanks' balanced salt solution and used for subsequent studies.

*Histology*

Formalin-fixed kidney samples were dehydrated through a graded ethanol series and embedded in Histosec (Merck, Darmstadt, Germany). Three-micrometer-thick sections were deparaffinized with xylene and rehydrated through a graded ethanol series. For conventional histopathological evaluation, kidney sections were stained with periodic acid Schiff.

*Electron Microscopy*

Blocks of renal cortex (1-mm cubes) were fixed in 2.5% (v/v) phosphate-buffered glutaraldehyde for 2 h, washed with phosphate buffer and postfixed in 1% (w/v) phosphate-buffered osmium tetroxide for 1 h at 4°C. After dehydration through ascending grades of ethanol, they were embedded in Epon resin (TAAB, UK). Then, 60-nm-thick ultrathin sections were cut using a diamond knife (Diatome, Bienne, Switzerland) on an EM UC6 ultramicrotome (Leica, Vienna, Austria), mounted on copper grids and stained with 4% (w/v) uranyl acetate and 0.3% (w/v) lead citrate solutions. They were observed with a Hitachi H-7650 electron microscope (Hitachi, Tokyo, Japan) operating at an accelerating voltage of 80 kV.

*Determination of Podocyte Number*

Three-micrometer-thick paraffin sections were immunostained for WT-1. Briefly, the sections were treated by autoclaving in 0.01 M citric acid buffer at 121°C for 5 min and then incubated with anti-WT-1 rabbit polyclonal antibody (Santa Cruz Biotechnology, Santa Cruz, Calif., USA) for 2 h at room temperature (22–25°C). After this incubation, the sections were incubated with horseradish peroxidase-labeled Envision for rabbits (Dako, Glostrup, Denmark) at room temperature for 30 min. The sections were treated with 3,3′-diaminobenzidine tetrahydrochloride (Dako). After washing with water, the sections were counterstained with hematoxylin and mounted with Entellan (Merck). Podocytes from 20 glomeruli were counted from 5 individual mice. Data are presented as a percentage of wild-type values.

*Immunofluorescence*

The kidneys were rapidly frozen in dry ice-cooled isopentane. Five-micrometer-thick fresh-frozen sections were immunostained. The primary antibodies used were as follows: anti-Tencl rabbit polyclonal antibody (GeneTex, Irvine, Calif., USA), anti-COL4A2 and anti-COL4A5 rat monoclonal antibodies (Chondrex, Redmond, Wash., USA), anti-laminin α5 and anti-laminin β2 rabbit polyclonal antibodies (Sigma), anti-laminin α1 and anti-laminin γ1 rat monoclonal antibodies, anti-integrin α3 and anti-phosphorylated ILK (phospho-ILK) rabbit polyclonal antibodies (Millipore, Billerica, Mass., USA), anti-laminin β1 rat monoclonal antibody (Thermo Fisher Scientific, Waltham, Mass., USA), anti-nephrin rabbit polyclonal antibody (IBL, Fujioka, Japan), anti-α-actinin-4 rabbit polyclonal antibody (ImmunoGlobe, Himmelstadt, Germany), anti-CD2AP rabbit polyclonal antibodies, anti-integrin β1 hamster monoclonal antibody and anti-synaptopodin goat polyclonal antibody (Santa Cruz), and anti-ILK, anti-FAK and anti-phosphorylated FAK (phospho-FAK) rabbit polyclonal antibodies (Abcam, Cambridge, UK). Sections were fixed with cold acetone (–80°C), and after washing with PBS (pH 7.4), they were incubated with each specific antibody. They were then washed with PBS and incubated with secondary antibodies conjugated with Alexa Fluor® 488 or 594 (Invitrogen). Sections were examined with a microscope (Axioplan2, Carl Zeiss Vision, Munich, Germany).

*Immunoprecipitation*

After preclearing with normal IgG, glomerular lysates were incubated at 4°C with anti-Tencl (Sigma), anti-integrin β1 (Santa Cruz), anti-ILK (Abcam) or anti-FAK (Abcam) antibodies, followed by precipitation with 30 μl of Protein A/G Plus-Agarose (Santa Cruz) at 4°C.

*Western Blotting*

The immunoprecipitated samples and the glomerular samples isolated from D2 and D2GN mice were electrophoresed on SDS-polyacrylamide gels, and separated proteins were transferred to Immobilon-P membranes (Millipore). The membranes were incubated with anti-Tencl (Sigma), anti-nephrin (IBL), anti-CD2AP, anti-synaptopodin (Santa Cruz), anti-α-actinin-4 (ImmunoGlobe) and anti-glyceraldehyde-3-phosphate dehydrogenase mouse monoclonal (Millipore) antibodies. Then, the membranes were washed and incubated with horseradish peroxidase-conjugated goat anti-rabbit IgG, anti-mouse IgG or rabbit anti-goat IgG antibodies (Dako) diluted at 1:2,000 at room temperature. After a wash, chemiluminescence was visualized using an electrochemiluminescence system (GE Healthcare, UK) according to the manufacturer's protocol. Similar experiments were performed at least 3 times. Chemiluminescence was recorded with a digital recorder (LAS-3000, Fujifilm), and then protein expression levels were quantified using ImageGauge (Fujifilm).

*Statistical Analysis*

Distributed data were expressed as mean values ± SD (n = 6 in each group) and assessed for significance by Student's t test using Microsoft Excel on a Macintosh computer. Differences at a probability of $p < 0.05$ were considered significant.

## Results

*Clinical Features*

We produced congenic strains by introducing the *Tencl* mutation of the ICGN strain into 2 genetic backgrounds, B6 and D2, by 12 generations of backcrossing. N12 mice were then intercrossed to generate *Tencl*$^{ICGN}$ homozygous mice, and the phenotype of both congenic strains, B6GN and D2GN, was analyzed. Firstly, we kept mice up to 20 weeks of age, and the clinical parameters of the sera were analyzed. As shown in tables 1 and 2, renal hypertrophy, hypoalbuminemia, elevated creatinine levels and hypercholesterolemia were noted in D2GN mice but not in B6GN mice. Next, urine from both strains at different ages was analyzed by SDS-PAGE. Proteinuria was observed by 14 days of age in D2GN mice and increased progressively with age; however, B6GN mice were analyzed up to 40 weeks of age and did not exhibit any signs of proteinuria (fig. 1).

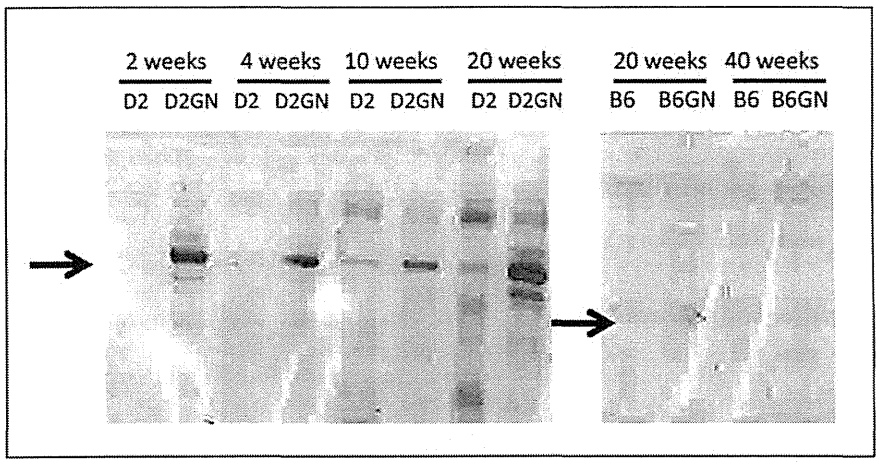


**Fig. 1.** Severe proteinuria in D2GN but not B6GN mice. Urine from both congenic and normal control strains at different time points was analyzed by SDS-PAGE. One microliter of urine from each mouse was loaded onto a 10% polyacrylamide gel. Proteinuria was observed at 14 days of age in D2GN mice and increased substantially with age. B6GN mice were analyzed up to 12 months of age and did not exhibit proteinuria. The arrows indicate the albumin bands.

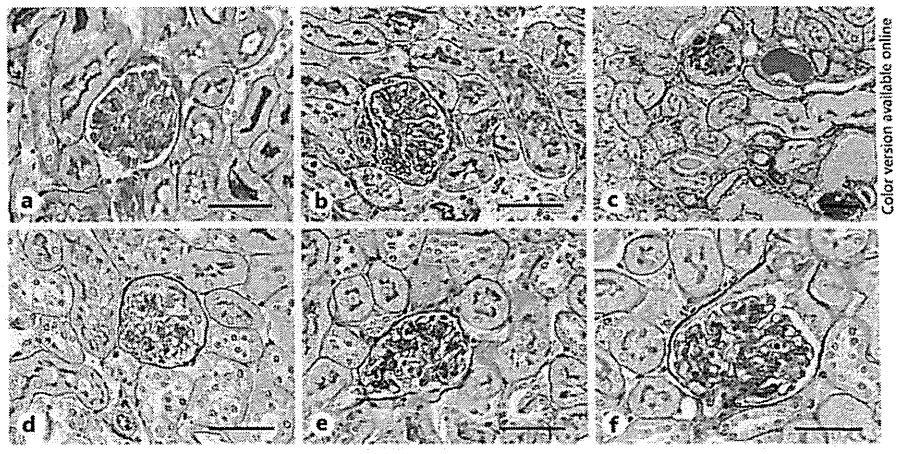


**Fig. 2.** Kidneys from both D2GN and B6GN strains were analyzed by periodic acid Schiff staining. **a–c** Compared with the kidney from a D2 mouse (**a**), the GBM of a D2GN mouse at 4 weeks (**b**) was slightly thickened. **c** At 14 weeks of age, glomerulosclerosis, tubular dilations and protein casts were observed in the D2GN kidney. **d–f** Some glomeruli at 20 and 40 weeks of age in B6GN mice showed mild mesangial expansion (**e**, **f**, respectively) compared with B6 mice (**d**). Scale bars = 50 μm.

**Table 1.** Body weight and relative kidney weight in the mice used

| Parameter | D2 | D2GN | B6 | B6GN |
|---|---|---|---|---|
| Body weight, g | 26.44±3.91 | 26.03±1.67 | 28.57±1.76 | 27.58±1.30 |
| Kidney weight/ body weight, % | 1.81±0.09 | 2.14±0.07* | 1.20±0.09 | 1.22±0.08 |

* $p < 0.05$ compared to D2.

**Table 2.** Serum biochemical features in D2GN and B6GN mice

| Parameter | D2 | D2GN | B6 | B6GN |
|---|---|---|---|---|
| Albumin, g/dl | 2.18±0.15 | 1.91±0.16* | 2.33±0.16 | 2.26±0.15 |
| Creatinine, mg/dl | 0.10±0.04 | 0.28±0.10* | 0.16±0.07 | 0.13±0.04 |
| BUN, mg/dl | 23.24±2.47 | 31.43±9.44 | 27.19±1.58 | 26.74±2.64 |
| Total cholesterol, mg/dl | 90.83±19.00 | 191.33±65.02* | 83.71±7.12 | 85.86±11.06 |

* $p < 0.05$ compared to D2. BUN = Blood urea nitrogen.

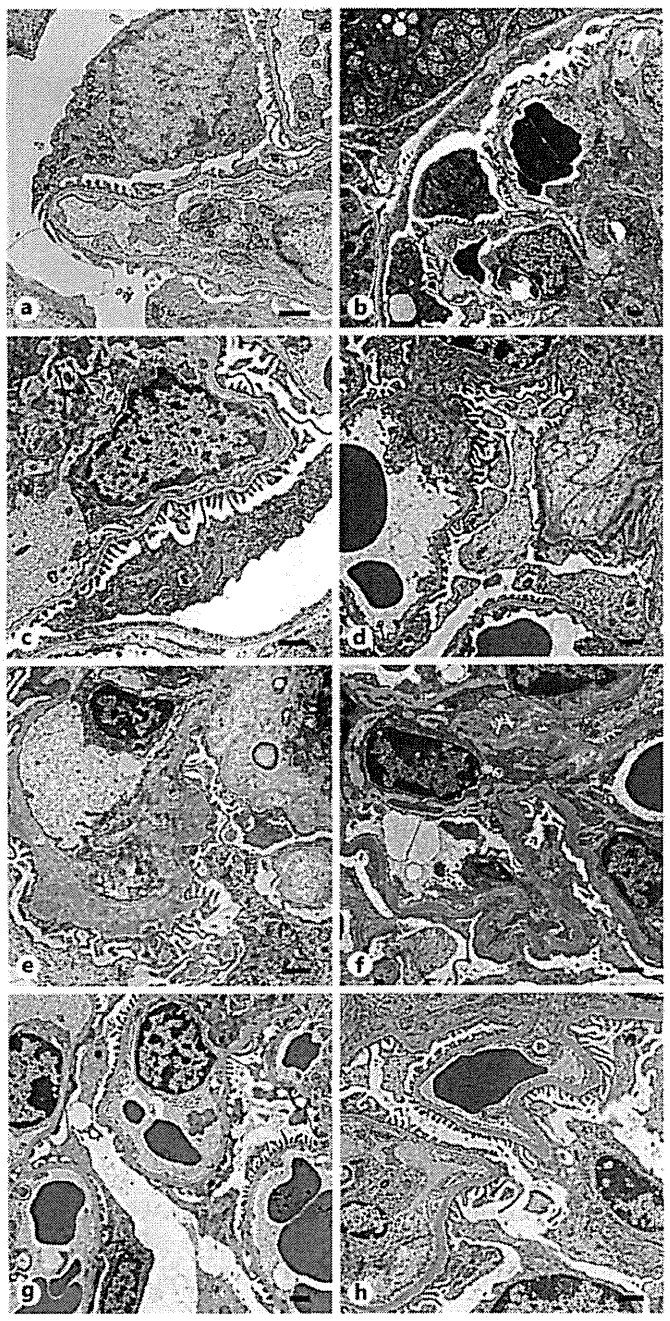

**Fig. 3.** TEM analysis of D2GN and B6GN strains. **a** D2 at 14 days. **b** D2GN at 14 days. **c** D2 at 4 weeks. **d** D2GN at 4 weeks. **e** D2GN at 10 weeks. **f** D2GN at 20 weeks. **g** B6 at 40 weeks. **h** B6GN at 40 weeks.TEM analysis showed that nodular thickening in the GBM of D2GN mice was apparent at 14 days (**b**), and GBM disorganization became more important at 4 weeks (**d**). The GBM was homogeneously thickened, and foot processes were partially effaced (**d**, **e**). **f** The thickened GBM and flattened foot processes were still seen at 20 weeks. **h** The GBM was slightly thickened in some glomeruli in B6GN mice at 40 weeks, but a normal structure of the glomerular filtration barrier was seen in most of the glomeruli. Scale bars = 1 μm.

*Renal Histopathology*

We performed periodic acid Schiff staining of both strains at different ages to assess the histopathological changes in GBM glomeruli. In some glomeruli of D2GN mice, slight thickening of the GBM was observed at 4 weeks of age (fig. 2a, b). The GBM thickening of D2GN mice became more severe with age, and enlargement of the mesangial region was observed by 8 weeks of age. In addition to glomerular defects, tubular injury occurs at around 14 weeks of age in the kidneys of D2GN mice (fig. 2c). The kidneys of B6GN mice up to 40 weeks of age (fig. 2d–f) and some glomeruli of 40-week-old B6GN mice showed mild mesangial expansion due to aging (fig. 2f). No remarkable injury was detected in the kidneys of B6GN mice.

*Ultrastructural Analysis*

To further elucidate morphological changes in the kidneys of D2GN mice, we performed ultrastructural analysis of glomeruli by transmission electron microscopy (TEM). GBM thickening was observed at 14 days of age in D2GN mice (fig. 3a, b), and then effacement of foot processes was partially observed at 4 weeks of age (fig. 3c, d). The degree of morphological changes in the GBM and podocytes progressively increased with age (fig. 3e, f), whereas podocyte detachment was not observed. In contrast, we also investigated the kidneys of B6GN mice up to 40 weeks of age, and slight GBM thickening was detected in a few glomeruli (fig. 3g, h).

*Defect in GBM Maturation*

GBM maturation normally occurs within the first 2 weeks after birth and involves a switch in the laminin and collagen IV networks. During initial GBM assembly, laminin-1 is expressed in the vascular clefts of early nephric figures but is eventually removed and replaced by laminin-11, which apparently is the only laminin present in the fully mature GBM [5]. Similarly, early GBMs contain COL4A1 and 4A2, but GBMs of fully mature glomeruli contain chiefly COL4A3–4A5 [5]. Thus, mature GBM is composed of COL4A3–4A5 and laminin-11. Since the TEM study showed thickening and splitting of the GBM in D2GN mice, we further investigated this GBM defect and whether it could reflect alterations in GBM assembly and maturation. Immunofluorescence analysis reveals that COL4A5 and laminin-11, which are components of the mature glomeruli, have a normal pattern of expression in the GBM of D2 and D2GN mice (fig. 4). COL4A2, the GBM component in immature glomeruli, is similarly expressed in the mesangium of D2 and D2GN mice,

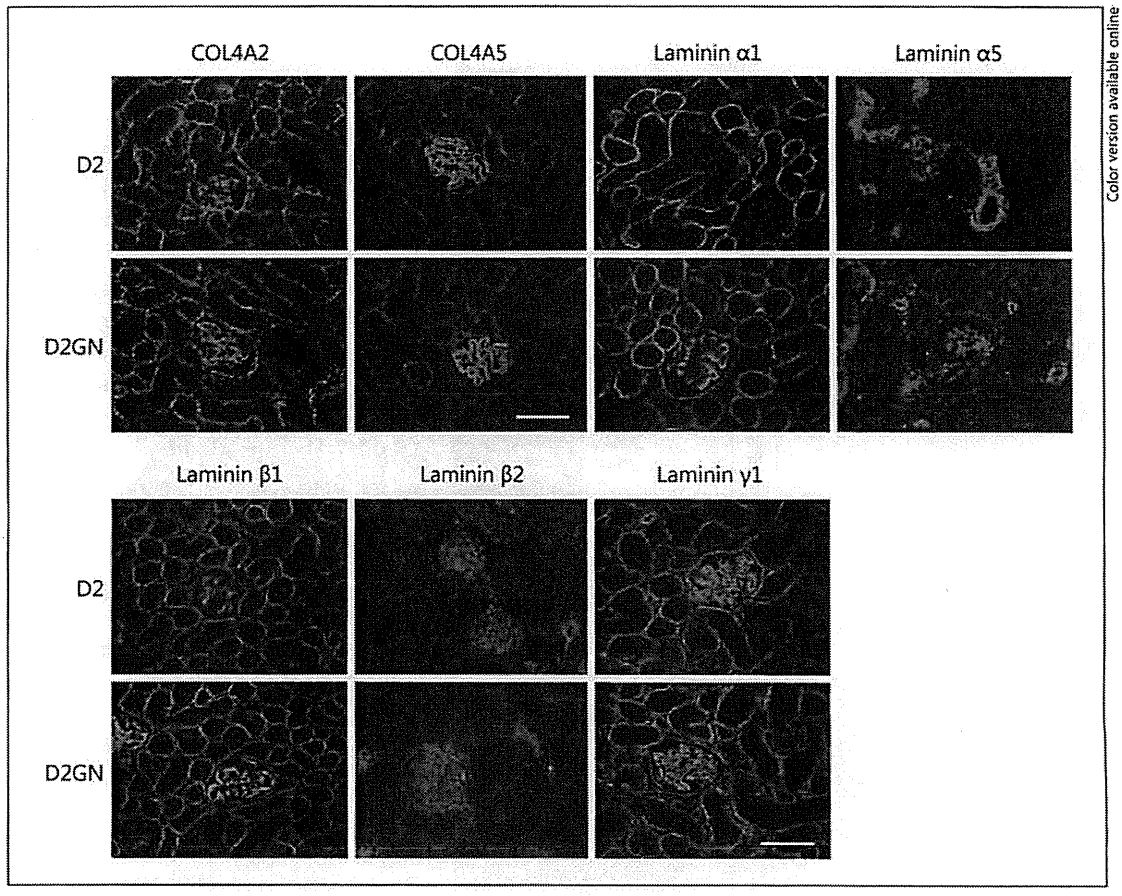


**Fig. 4.** Immunofluorescence study for collagen IV and laminin chains in different strains of mice at 3 weeks of age. The expression of COL4A2 and COL4A5 in D2GN mice was the same as in D2 mice. Laminin-11 (α5β2γ1) expression with a normal pattern was shown in the GBM of all groups. Laminin-1 (α1β1γ1), which is normally expressed in the mesangium of normal mature glomeruli but is absent in the GBM, was expressed in the GBM of D2GN mice. Scale bars = 50 μm.

whereas laminins α1 and β1, which are normally expressed in the mesangium of normal mature glomeruli but are absent in the GBM, were expressed in the GBM of 3-week-old D2GN mice (fig. 4). These results suggest that GBM components in immature glomeruli continue to be expressed in the GBM of mature glomeruli in D2GN mice.

*Podocyte Injury*

As described above, the TEM study indicated effacement of podocyte foot processes in the kidneys of D2GN mice after GBM abnormalities occurred. To estimate the podocyte number per glomerulus, we counted the number of immunohistochemically WT-1-positive cells in the glomeruli of 10- and 20-week-old mice. The numbers of WT-1-positive cells were markedly lower in D2GN mice than in D2 mice, but podocyte loss was not seen in B6GN mice (fig. 5a). To clarify that the deficiency of Tencl influences the slit diaphragm complexes and focal adhesion complexes between foot processes and the GBM, we further examined the distribution and abundance of podocyte-specific proteins in the kidneys of 10- and 20-week-old D2GN mice by immunofluorescence and Western blot (fig. 5b–d). Firstly, we observed that the expression of nephrin, a major component of slit diaphragm complexes, was lower in 10-week-old D2GN mice than in D2 mice. CD2AP is an actin-associated protein that interacts with nephrin and facilitates the selec-

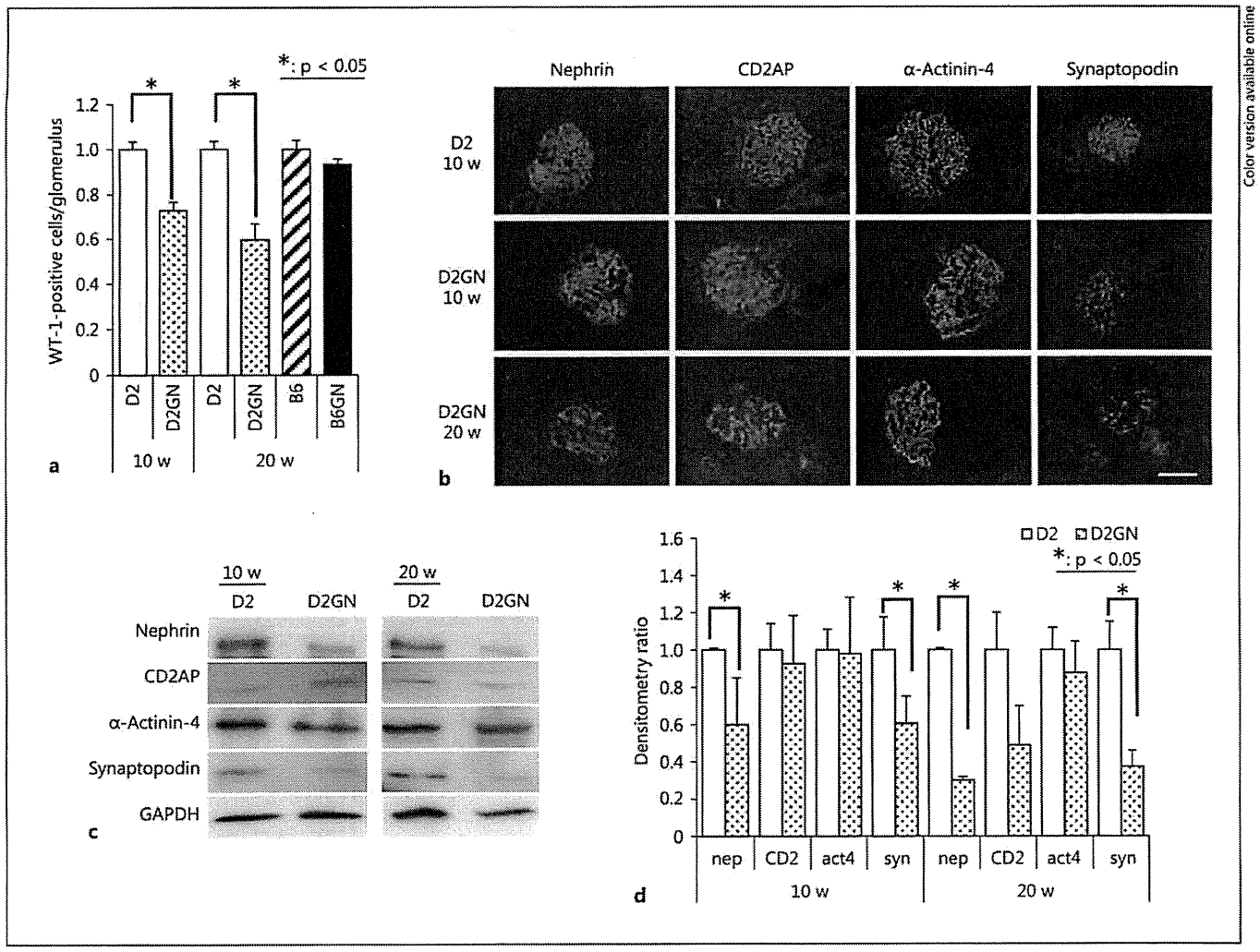


**Fig. 5.** Podocyte injury. **a** Podocyte number per glomerulus was estimated by counting nuclei positive for WT-1 staining. Results were normalized to the average podocyte number in the normal control. The numbers of WT-1-positive cells in D2GN mice were markedly lower than in D2 mice, but podocyte loss was not seen in B6GN mice. **b** Immunofluorescence staining for podocyte-specific proteins. The expression and localization of podocyte-specific proteins (nephrin, CD2AP, α-actinin-4 and synaptopodin) in the kidneys of D2 and D2GN mice are demonstrated. Scale bar = 50 μm. **c** Western blot analysis for podocyte-specific proteins (n = 4). GAPDH = Glyceraldehyde-3-phosphate dehydrogenase. **d** Mean densitometric analysis. The expression of nephrin and synaptopodin steadily decreased with age in glomeruli of D2GN mice.

tive recruitment of signaling molecules. The expression of CD2AP also decreased in D2GN mice with age. We observed that the expression of α-actinin-4, an actin-associated protein that links the slit diaphragm to the actin cytoskeleton, was not different between D2GN and D2 mice. Synaptopodin, a proline-rich actin-associated protein highly expressed in foot processes, was strongly expressed in podocytes of D2 mice, whereas the expression of synaptopodin was decreased in 10-week-old D2GN mice.

*Podocyte-GBM Interaction*

Podocytes adhere to the GBM principally via integrin α3β1, which acts as a receptor for laminin-10 and/or laminin-11. Alterations in integrin α3β1, which anchors podocyte foot processes to the GBM, also cause both GBM abnormalities and effacement of foot processes. Tencl is known to participate in integrin signaling by interacting with the cytoplasmic tail of integrin β1. We examined the expression of Tencl and integrin α3β1 by immunofluorescence staining. As previously reported [18],

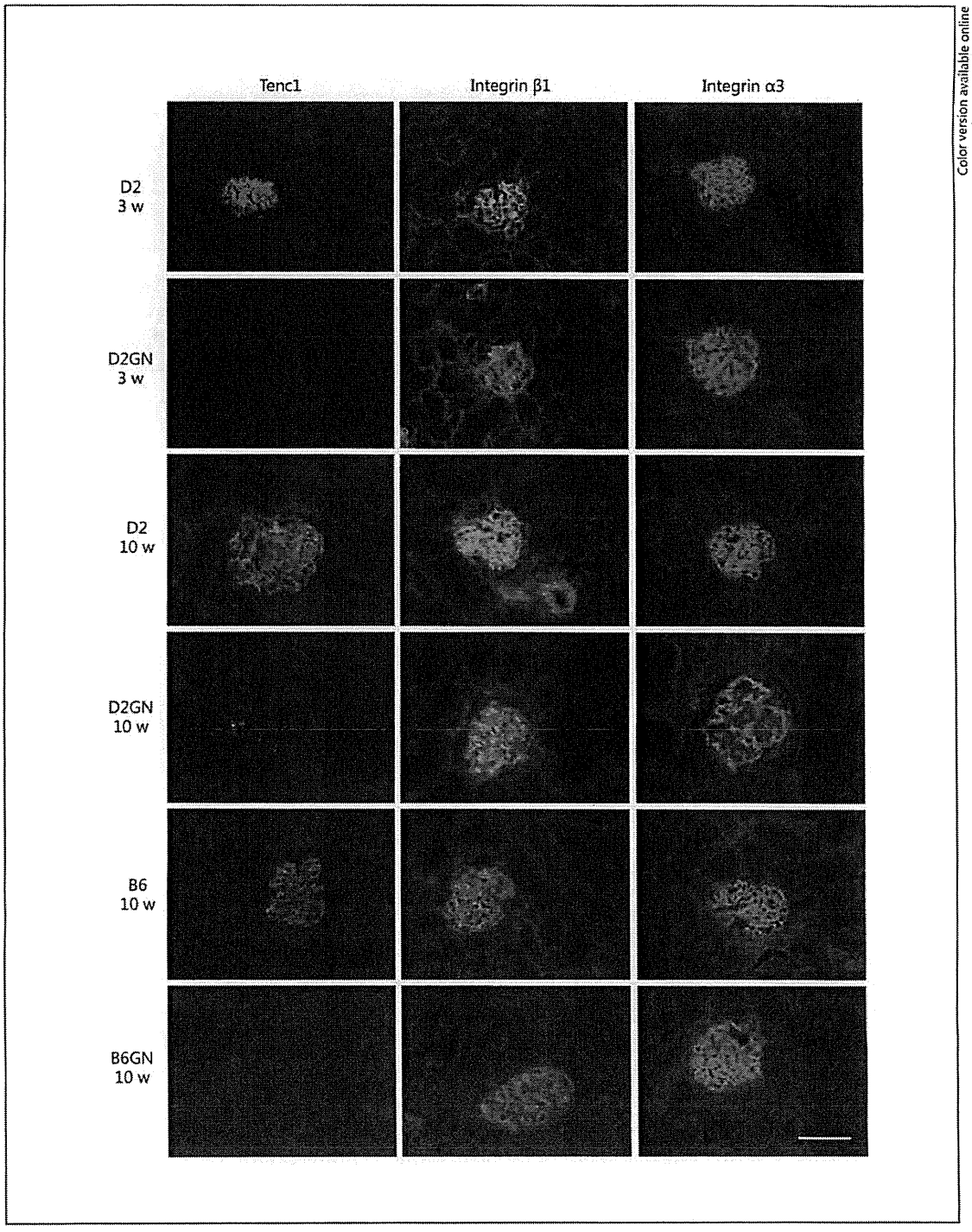


Color version available online

**Fig. 6.** Immunofluorescence study for Tencl and integrin α3β1 in the kidneys of D2GN and B6GN mice. Tencl is not expressed in the kidneys of *Tencl* mutant mice. Integrin β1 is expressed in the same pattern in all strains. Integrin α3 was normally expressed in the kidneys of D2GN mice at 3 weeks of age but linearly expressed in the outermost podocyte layer of the capillary tuft in D2GN mice at 10 weeks of age. Scale bar = 50 μm.

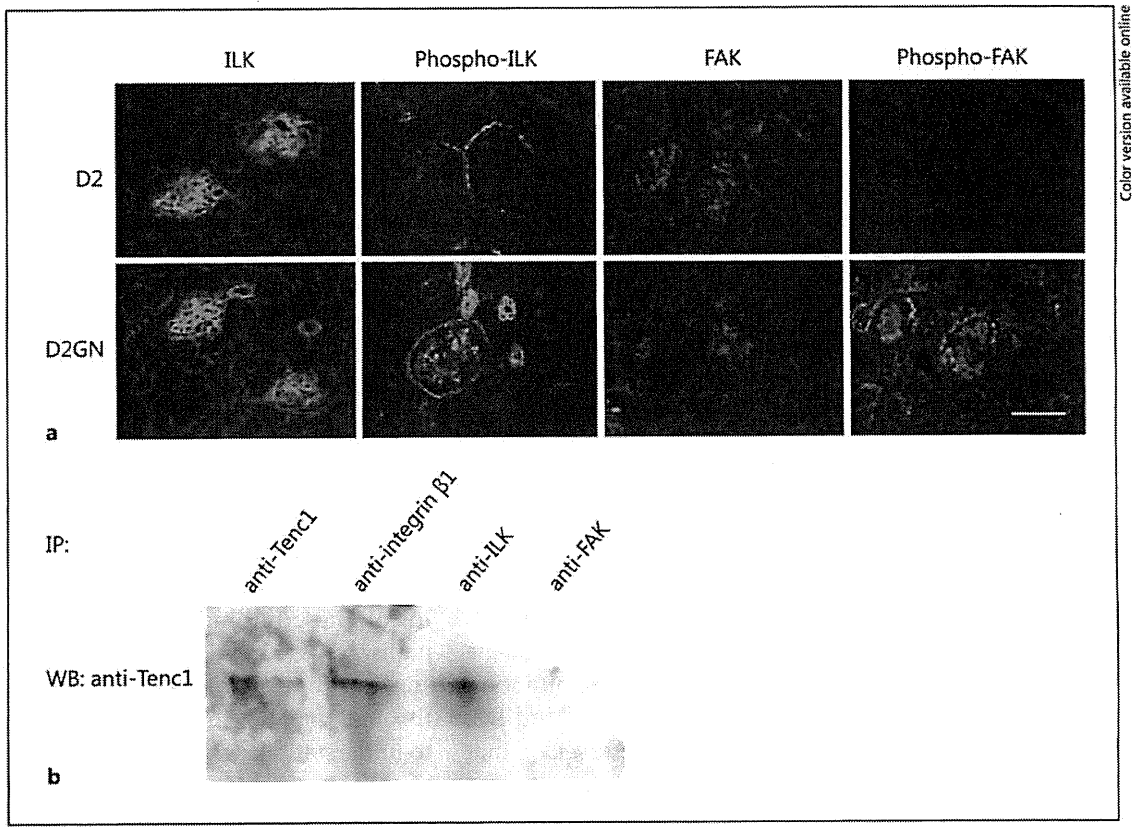


**Fig. 7.** Expression of the integrin signaling molecules ILK and FAK in D2 and D2GN mice. **a** Expression of ILK and FAK in the kidneys of D2 and D2GN mice at 3 weeks of age. There were no differences in the expression of ILK and FAK between D2 and D2GN mice, but phospho-ILK and phospho-FAK were noted in only D2GN mice. Scale bar = 50 μm. **b** Glomerular lysates were immunoprecipitated with anti-Tenc1, anti-integrin β1, anti-ILK and anti-FAK antibodies, followed by immunoblotting with an anti-Tenc1 antibody. IP = Immunoprecipitation; WB = Western blot.

Tenc1 is expressed in the podocytes of normal kidney but not in the kidneys of *Tenc1* mutant mice (fig. 6). An immunofluorescence study revealed that there was no difference in the expression of integrin β1 between normal and *Tenc1* mutant mice (fig. 6). By contrast, integrin α3 was normally expressed in 3-week-old D2GN mice but linearly expressed in the outermost podocyte layer of the capillary tuft in 10-week-old D2GN mice (fig. 6). This abnormal expression of integrin α3 may be caused by mesangial expansion. The normal pattern of integrin α3 expression was observed in B6 and B6GN glomeruli (fig. 6).

*Integrin Signaling*

Integrins possess no enzymatic or actin-binding activity of their own and thus act as adaptor molecules like Tenc1. Through interaction with signal molecules, integrin transduces signals and regulates biological functions. ILK and FAK are important signaling intermediates of integrin β1, and these proteins have different downstream effector molecules. ILK, a serine/threonine protein kinase, interacts with the cytoplasmic domains of β integrins and regulates integrin functions [13]. FAK, a nonreceptor tyrosine kinase, requires integrin-induced autophosphorylation at tyrosine 397, resulting in activation of critical signaling pathways for focal adhesion turnover [14]. FAK controls actin reorganization and cell-cell or cell-matrix adhesion downstream of integrin β1. We examined whether 2 proximal integrin β1 signaling intermediates, ILK and FAK, contribute to glomerular defects by the loss of Tenc1, an integrin signaling molecule. Immunofluorescence staining demonstrated that there was no difference noted in the expression of ILK and FAK

between 3-week-old D2GN and D2 mice, but phospho-ILK and phospho-FAK were seen in the glomeruli of D2GN mice only (fig. 7a). We then examined the potential interaction between ILK, FAK and Tencl in glomeruli by immunoprecipitation analysis. As shown in figure 7b, Tencl was detected in the complex that was precipitated by the anti-ILK antibody, not anti-FAK, suggesting that Tencl activates ILK directly and FAK indirectly and influences integrin signaling.

## Discussion

Tencl, an integrin-mediated focal adhesion molecule, is widely expressed in mouse tissues [19]. Recently, it was demonstrated that the ICGN mouse, a nephrotic syndrome model, has mutated *Tencl* [18]. Tencl is mainly expressed in the podocytes in normal mouse kidneys but not in ICGN kidneys [18]. To understand the mechanisms underlying the development of kidney diseases and the roles of Tencl in kidney disease, a *Tencl*$^{ICGN}$ mutation was introduced into 2 genetic backgrounds, B6 and D2. The phenotypic analyses of *Tencl*$^{ICGN}$ mice revealed that D2GN mice developed nephrotic syndrome, whereas B6GN mice did not. The present findings imply that the development of nephrotic syndrome due to the *Tencl* mutation is dependent on the genetic background. The B6 strain is known to be relatively resistant to kidney diseases, in comparison to other strains [26–29]. For example, *COL4A3* knockout mice, a model of Alport syndrome, exhibited more severe GBM damage on a 129/Sv background than on a B6 background [28, 29]. Further, mice deficient for CD151, associated with integrin α3β1, displayed a GBM abnormality on an FVB background but were healthy on a B6 background [27]. In contrast, mice deficient for podocin, the slit diaphragm-associated protein, developed more severe glomerular disease on a B6 background than on a 129/Sv background [30]. These findings mean that the modifier genes associated with defects of the slit diaphragm protein are distinct from those related to defects of GBM components and GBM-podocyte interaction [27]. In the present study, mice deficient for Tencl displayed thickening of the GBM shortly after birth on a D2 background, whereas such abnormality was not observed on a B6 background, and the deficit in the GBM on a D2 background probably leads to podocyte dysfunction. These mouse strains allow us to identify the modifier genes influencing the onset of glomerular disease. Hence, we generated an F2 hybrid, i.e. F1 (B6GN × D2GN) × D2GN, and started a quantitative trait locus analysis.

TEM observation revealed that the initial manifestation of *Tencl* mutant mice was an abnormality of the GBM, and the effacement of podocyte foot processes was observed following GBM defects. During the early stage of glomerular development, laminin-1 is synthesized but is finally removed and replaced by laminin-11, which is the only laminin present in the mature GBM [5]. Similar shifts occur in collagen IV [5]. In this study, we showed that the mature GBM in *Tencl* mutant mice contained both laminin α1 and β1 chains, which are immature GBM components. Coexpression of mature and immature components in the GBM suggests a defect in GBM assembly and maturation. Several studies have demonstrated that integrin β1 is required for the proper assembly of basement membranes [16]. In addition, the persistence of laminin β1 in the GBM of mature glomeruli of podocyte-specific ILK-deficient mice [15, 16] and CD151-deficient mice [27] has been reported, as observed in *Tencl* mutant mice. These findings indicate that integrin downstream pathways also regulate GBM assembly. Our present study suggests that Tencl likely participates in GBM assembly through the integrin pathway. Further studies are needed to understand how Tencl regulates the change in expression of integrin β1 downstream molecules.

We observed podocyte architecture in *Tencl* mutant mice by TEM and immunohistochemical staining. Effacement of podocyte foot processes occurs following GBM disorganization, and the expression of podocyte-specific proteins decreased with age in *Tencl* mutant mice. It is known that the abnormal organization of the GBM may lead to increased permeability and exposure of podocytes to atypical hemodynamic forces [31], so that the hemodynamic pressure soon after birth in an abnormal GBM structure probably leads to podocyte injury in *Tencl* mutant mice. In addition, integrin signaling influences not only GBM assembly but also podocyte architecture [13, 14]. The major integrin downstream molecules, ILK and FAK, are known to regulate podocyte structure [13–16]. ILK interacts with the cytoplasmic domains of integrin β and with nephrin in the podocyte, and the integrin signals in the podocyte are intrinsically coupled through an ILK-dependent mechanism [15]. In contrast, phosphorylation of FAK at tyrosine 397 following integrin engagement results in activation of signaling pathways related to focal adhesion turnover, and FAK activation regulates foot process effacement in the podocyte [15, 16]. Further, it has been demonstrated that phospho-FAK is induced in podocyte-specific ILK-deficient mice but not in podocyte-specific integrin β1-deficient mice [15, 16]. In this study, a normal expression pattern of in-

tegrin β1 was observed in *Tencl* mutant mice, whereas the expression levels of phospho-ILK and phospho-FAK were markedly increased. Additionally, immunoprecipitation analysis revealed that Tencl might interact with ILK and integrin β1 in glomeruli, but not with FAK. Collectively, Tencl may act downstream of integrin β1 through ILK signaling to regulate GBM assembly and formation of podocyte foot processes. ILK regulates slit diaphragm signals, but it remains unclear whether Tencl relates to these signals. Further studies are needed to investigate integrin-ILK-Tencl signals. Tencl is a cytoplasmic phosphoprotein that is localized to integrin-mediated focal adhesions [19, 20]. Tencl contains PTB and SH2 domains at the C terminus that interact with tyrosine-phosphorylated proteins, PKC and actin-binding domains at the N terminus, but the center region of Tencl does not contain the actin-capping domain present in tensin1, suggesting that it is not able to regulate actin polymerization [19–22]. In addition, Tencl has a phosphatase and a C2 domain pairing, which is homologous to phosphatase and the tensin homolog [19–22]. The tensin family, which is known to be a metastasis suppressor, can inhibit cell proliferation and migration, and its expression is strongly downregulated in human cancers [32]. In particular, it is known that Tencl influences the phosphoinositide 3-kinase (PI3K)/Akt signaling pathway and enhances apoptosis in addition to inhibiting cell migration in cancers [21]. In podocytes, it is known that activation of the PI3K/Akt pathway by nephrin or CD2AP protects against apoptosis and is involved in actin reorganization [33, 34]. Further study is required to determine whether Tencl participates in glomerular PI3K/Akt pathways, and identifying molecules that interact with Tencl in podocytes may help to understand the mechanism of glomerular injury.

In conclusion, *Tencl* mutant mice develop nephrotic syndrome dependent on the genetic background, and the mutant strain on the D2 background, but not the B6 background, is a useful model for human idiopathic nephrotic syndrome. Identifying modifier genes may help to understand the mechanism of nephrotic syndrome and additionally to define the cause of B6GN resistance to glomerular defects, and the molecular mechanism of compensation may assist in the development of new treatments. The present study sheds light on the involvement of Tencl in glomerular integrin signaling and contributes to clarify the contribution of Tencl to the organization of the GBM structure.


## Acknowledgements

This work was supported by a Grant-in-Aid for Scientific Research from the Japan Society for the Promotion of Science and a grant from the Ministry of Health, Labor and Welfare, Japan. We thank Dr. Takayoshi Imazawa for excellent assistance with electron microscopes.


## Disclosure Statement

None of the authors have competing interests to declare.

## References


1 Caridi G, Trivelli A, Sanna-Cherchi S, Perfumo F, Ghiggeri GM: Familial forms of nephrotic syndrome. Pediatr Nephrol 2010;25:241–252.
2 Machuca E, Benoit G, Antignac C: Genetics of nephrotic syndrome: connecting molecular genetics to podocyte physiology. Hum Mol Genet 2009;18:R185–R194.
3 Jalanko H: Congenital nephrotic syndrome. Pediatr Nephrol 2009;24:2121–2128.
4 Tryggvason K, Patrakka J, Wartiovaara J: Hereditary proteinuria syndromes and mechanisms of proteinuria. N Engl J Med 2006;354:1387–1401.
5 Miner JH: Renal basement membrane components. Kidney Int 1999;56:2016–2024.
6 Harvey SJ, Zheng K, Sado Y, Naito I, Ninomiya Y, Jacobs RM, Hudson BG, Thorner PS: Role of distinct type IV collagen networks in glomerular development and function. Kidney Int 1998;54:1857–1866.
7 Miner JH, Go G, Cunningham J, Patton BL, Jarad G: Transgenic isolation of skeletal muscle and kidney defects in laminin β2 mutant mice: implications for Pierson syndrome. Development 2006;133:967–975.
8 Noakes PG, Miner JH, Gautam M, Cunningham JM, Sanes JR, Merlie JP: The renal glomerulus of mice lacking s-laminin/laminin β2: nephrosis despite molecular compensation by laminin β1. Nat Genet 1995;10:400–406.
9 Cosgrove D, Meehan DT, Grunkemeyer JA, Kornak JM, Sayers R, Hunter WJ, Samuelson GC: Collagen COL4A3 knockout: a mouse model for autosomal Alport syndrome. Genes Dev 1996;10:2981–2992.
10 Kestilä M, Lenkkeri U, Männikkö M, Lamerdin J, McCready P, Putaala H, Ruotsalainen V, Morita T, Nissinen M, Herva R, Kashtan CE, Peltonen L, Holmberg C, Olsen A, Tryggvason K: Positionally cloned gene for a novel glomerular protein – nephrin – is mutated in congenital nephrotic syndrome. Mol Cell 1998;1:575–582.
11 Boute N, Gribouval O, Roselli S, Benessy F, Lee H, Fuchshuber A, Dahan K, Gubler MC, Niaudet P, Antignac C: NPHS2, encoding the glomerular protein podocin, is mutated in autosomal recessive steroid-resistant nephrotic syndrome. Nat Genet 2000;24:349–354.

12 Kreidberg JA, Donovan MJ, Goldstein SL, Rennke H, Shepherd K, Jones RC, Jaenisch R: α3β1 integrin has a crucial role in kidney and lung organogenesis. Development 1996;122:3537–3547.
13 Dai C, Stolz DB, Bastacky SI, St-Arnaud R, Wu C, Dedhar S, Liu Y: Essential role of integrin-linked kinase in podocyte biology: bridging the integrin and slit diaphragm signaling. J Am Soc Nephrol 2006;17:2164–2175.
14 Ma H, Togawa A, Soda K, Zhang J, Lee S, Ma M, Yu Z, Ardito T, Czyzyk J, Diggs L, Joly D, Hatakeyama S, Kawahara E, Holzman L, Guan JL, Ishibe S: Inhibition of podocyte FAK protects against proteinuria and foot process effacement. J Am Soc Nephrol 2010;21:1145–1156.
15 El-Aouni C, Herbach N, Blattner SM, Henger A, Rastaldi MP, Jarad G, Miner JH, Moeller MJ, St-Arnaud R, Dedhar S, Holzman LB, Wanke R, Kretzler M: Podocyte-specific deletion of integrin-linked kinase results in severe glomerular basement membrane alterations and progressive glomerulosclerosis. J Am Soc Nephrol 2006;17:1334–1344.
16 Kanasaki K, Kanda Y, Palmsten K, Tanjore H, Lee SB, Lebleu VS, Gattone VH Jr, Kalluri R: Integrin β1-mediated matrix assembly and signaling are critical for the normal development and function of the kidney glomerulus. Dev Biol 2008;313:584–593.
17 Ogura A, Asano T, Matsuda J, Takano K, Nakagawa M, Fukui M: Characteristics of mutant mice (ICGN) with spontaneous renal lesion: a new model for human nephrotic syndrome. Lab Anim 1989;23:169–174.
18 Cho A-R, Uchio-Yamada K, Torigai T, Miyamoto T, Miyoshi I, Matsuda J, Kurosawa T, Kon Y, Asano A, Sasaki N, Agui T: Deficiency of the tensin2 gene in the ICGN mouse, an animal model for congenital nephrotic syndrome. Mamm Genome 2006;17:407–416.
19 Chen H, Duncan IC, Bozorgchami H, Lo SH: Tensin1 and a previously undocumented family member, tensin2, positively regulate cell migration. Proc Natl Acad Sci USA 2002;99:733–738.
20 Lo SH: Tensin. Int J Biochem Cell Biol 2004;36:31–34.
21 Hafizi S, Gustafsson A, Oslakovic C, Idevall-Hagren O, Tengholm A, Sperandio O, Villoutreix BO, Dahlbäck B: Tensin2 reduces intracellular phosphatidylinositol 3,4,5-trisphosphate levels at the plasma membrane. Biochem Biophys Res Commun 2010;399:396–401.
22 Hafizi S, Sernstad E, Swinny JD, Gomez MF, Dahlbäck B: Individual domains of Tensin2 exhibit distinct subcellular localisations and migratory effects. Int J Biochem Cell Biol 2010;42:52–61.
23 Nishino T, Sasaki N, Nagasaki K, Ahmad Z, Agui T: Genetic background strongly influences the severity of glomerulosclerosis in mice. J Vet Med Sci 2010;72:1313–1318.
24 Kato T, Mizuno-Horikawa Y, Mizuno S: Decreases in podocin, CD2-associated protein (CD2AP) and tensin2 may be involved in albuminuria during septic acute renal failure. J Vet Med Sci 2011;73:1579–1584.
25 Takemoto M, Asker N, Gerhardt H, Lundkvist A, Johansson BR, Saito Y, Betsholtz C: A new method for large scale isolation of kidney glomeruli from mice. Am J Pathol 2002;161:799–805.
26 Sheehan S, Tsaih SW, King BL, Stanton C, Churchill GA, Paigen B, DiPetrillo K: Genetic analysis of albuminuria in a cross between C57BL/6J and DBA/2J mice. Am J Physiol Renal Physiol 2007;293:F1649–F1656.
27 Baleato RM, Guthrie PL, Gubler MC, Ashman LK, Roselli S: Deletion of CD151 results in a strain-dependent glomerular disease due to severe alterations of the glomerular basement membrane. Am J Pathol 2008;173:927–937.
28 Andrews KL, Mudd JL, Li C, Miner JH: Quantitative trait loci influence renal disease progression in a mouse model of Alport syndrome. Am J Pathol 2002;160:721–730.
29 Kang JS, Wang XP, Miner JH, Morello R, Sado Y, Abrahamson DR, Borza DB: Loss of α3/α4 (IV) collagen from the glomerular basement membrane induces a strain-dependent isoform switch to α5α6 (IV) collagen associated with longer renal survival in Col4a3–/– Alport mice. J Am Soc Nephrol 2006;17:1962–1969.
30 Roselli S, Heidet L, Sich M, Henger A, Kretzler M, Gubler MC, Antignac C: Early glomerular filtration defect and severe renal disease in podocin-deficient mice. Mol Cell Biol 2004;24:550–560.
31 Jarad G, Cunningham J, Shaw AS, Miner JH: Proteinuria precedes podocyte abnormalities in Lamb2–/– mice, implicating the glomerular basement membrane as an albumin barrier. J Clin Invest 2006;116:2272–2279.
32 Chan LK, Ko FC, Ng IO, Yam JW: Deleted in liver cancer 1 (DLC1) utilizes a novel binding site for tensin2 PTB domain interaction and is required for tumor-suppressive function. PLoS One 2009;4:e5572.
33 Zhu J, Sun N, Aoudjit L, Li H, Kawachi H, Lemay S, Takano T: Nephrin mediates actin reorganization via phosphoinositide 3-kinase in podocytes. Kidney Int 2008;73:556–566.
34 Huber TB, Hartleben B, Kim J, Schmidts M, Schermer B, Keil A, Egger L, Lecha RL, Borner C, Pavenstädt H, Shaw AS, Walz G, Benzing T: Nephrin and CD2AP associate with phosphoinositide 3-OH kinase and stimulate AKT-dependent signaling. Mol Cell Biol 2003;23:4917–4928.

Original Paper

nephron
Experimental
Nephrology

Nephron Exp Nephrol 2013;123:34–45
DOI: 10.1159/000354057

Received: January 4, 2013
Accepted: June 26, 2013
Published online: August 23, 2013

# Gene Expression Analysis Detected a Low Expression Level of *C1s* Gene in ICR-Derived Glomerulonephritis (ICGN) Mice

Kotaro Tamura[a] Kozue Uchio-Yamada[b] Noboru Manabe[c] Takahisa Noto[a]
Rika Hirota[a] Akira Unami[a] Masahiro Matsumoto[a] Yoichi Miyamae[a]

[a]Drug Safety Research Laboratories, Astellas Pharma Inc., Osaka, [b]Laboratory of Animal Models for Human Diseases, National Institute of Biomedical Innovation, Ibaraki, and [c]Animal Resource Center, The University of Tokyo, Kasama, Japan

**Key Words**
ICR-derived glomerulonephritis mice · ICGN strain · *C1s* gene · Gene expression

**Abstract**
***Background:*** ICR-derived glomerulonephritis (ICGN) strain is a novel inbred strain of mice with a hereditary nephrotic syndrome. Deletion mutation of tensin 2 *(Tns2)*, a focal adhesion molecule, has been suggested to be responsible for nephrotic syndrome in ICGN mice; however, the existence of other associative factors has been suggested. ***Methods and Results:*** To identify additional associative factors and to better understand the onset mechanism of nephrotic syndrome in ICGN mice, we conducted a comprehensive gene expression analysis using DNA microarray. Immune-related pathways were markedly altered in ICGN mice kidney as compared with ICR mice. Furthermore, the gene expression level of complement component 1, s subcomponent *(C1s)*, whose human homologue has been reported to associate with lupus nephritis, was markedly low in ICGN mouse kidney. Real-time quantitative reverse transcription-polymerase chain reaction confirmed a low expression level of *C1s* in ICGN mouse liver where the C1s protein is mainly synthesized. A high serum level of anti-dsDNA antibody and deposits of immune complexes were also detected in ICGN mice by enzyme-linked immunosorbent assay and immunohistochemical analyses, respectively. ***Conclusion:*** Our results suggest that the immune system, especially the complement system, is associated with nephrotic syndrome in ICGN mice. We identified a low expression level of *C1s* gene as an additional associative factor for nephrotic syndrome in ICGN mice. Further studies are needed to elucidate the role of the complement system in the onset of nephrotic syndrome in ICGN mice.



## Introduction

Hereditary spontaneous nephrotic mice (ICGN mice), a novel mutant mouse strain derived from the ICR strain, were established in the National Institute of Infectious Diseases [1, 2]. ICGN mice show proteinuria at a young age and develop severe hypoproteinemia and hyperlipidemia, while some of the mice also develop systemic edema [3]. Histopathological analyses of ICGN mice kidney showed glomerular lesions consisting of thickened glomerular basement membrane (GBM) with irregular

KARGER

E-Mail karger@karger.com
www.karger.com/nee


1660–2129/13/1234–0034$38.00/0

Kotaro Tamura
Drug Safety Research Laboratories, Astellas Pharma Inc.
2-1-6, Kashima, Yodogawa-ku
Osaka 532-8514 (Japan)
E-Mail kotaro.tamura@astellas.com

spike-like protrusions and enlargement of the mesangial area without cellular proliferation [2]. Ultrastructurally, multilaminar splitting of the lamina densa of the thickened GBM and fusion of the epithelial foot processes were noted [4–6]. Such ultrastructural glomerular alterations were already observed in the kidneys of neonatal ICGN mice (4–6 days after birth) [6].

The proteinuria seen in ICGN mice was reported to be controlled by at least one autosomal recessive gene *(nep)*, which was mapped on the distal part of chromosome 15 by linkage analysis [7]. In addition, quantitative trait locus analysis and DNA sequencing raised the possibility that a deletion mutation of tensin 2 (*Tns2*), also located on chromosome 15, was responsible for nephrotic syndrome in ICGN mice [8]. Tensin is a focal adhesion molecule that binds to actin filaments and participates in signaling pathway through integrin [9]. The *Tns2* gene was reported as *Tenc1*, tensin-like C1 domain containing phosphatase, in Mouse Genome Informatics (http://www.informatics.jax.org/). While *Tns2* is expressed in podocytes and tubular epithelial cells in normal mice, the deletion mutation in *Tns2* creates a premature terminal codon in ICGN mice [8]. Although the deletion mutation of *Tns2* was suggested to be responsible for nephrotic syndrome in ICGN mice, some reports have suggested existence of other causative factors. Backcross progenies of (ICGN × MSM)$F_1$ × ICGN showed various degrees of proteinuria but did not segregate into the ICGN and MSM types [8]. This result indicates that proteinuria is controlled by multiple genetic loci. Congenic strains carrying the mutation of *Tns2* on the C57BL/6J genetic background showed milder phenotypes than ICGN mice [10]. Additionally, congenic strains carrying the mutation of *Tns2* on the 129/SV genetic background did not show proteinuria, anemia, increase in blood urea nitrogen (BUN) or any severe histological changes until at least 16 weeks of age [11]. These results suggest the absence of nephrotic syndrome in congenic strains carrying the mutation of *Tns2* on the C57BL/6J and the 129/SV genetic background was because they retained wild-type expression for the multiple associative factors involved in the nephrotic syndrome seen in ICGN mice.

To identify additional associative factors for nephrotic syndrome in ICGN mice and to better understand the onset mechanism of nephrotic syndrome in ICGN mice, microarray analysis was conducted on renal cortex from 4- and 8-week-old ICGN mice and the results were compared to those obtained from renal cortex harvested from ICR mice.

## Methods

*Animals and Tissue Preparation*

All animal experiments were performed in accordance with protocols approved by the Institutional Animal Care and Use Committees of National Institute of Biomedical Innovation (NIBIO, Osaka, Japan). Homozygous male ICGN mice (4 and 8 weeks old) from a specific pathogen-free colony at NIBIO and age-matched ICR mice (Clea Japan, Osaka, Japan) were used in this study. All animals were housed under environmentally controlled conditions (room temperature: 23 ± 1°C; light-dark conditions: 14 h light/10 h dark) in autoclaved cages and given a standard diet (CMF, Oriental Yeast Co., Tokyo, Japan) and tap water ad libitum. At 4 or 8 weeks of age, the animals were anesthetized, urine samples obtained from the bladder, blood samples from the cervical vein, and the kidneys and liver were rapidly removed. One kidney was immediately fixed in 10% (v/v) neutral-buffered formalin (pH 7.4) for conventional histopathological evaluation and immunohistochemical study while the other kidney was sectioned horizontally at its middle portion into approximately a 1-mm thick slice. The slices were fixed in RNA*later*® (Invitrogen, Carlsbad, Calif., USA) for microarray analysis. The median hepatic lobe was sectioned into approximately a 5-mm thick slice and then fixed in RNA*later*® for real-time quantitative reverse transcription-polymerase chain reaction (quantitative PCR).

*Clinical Biochemistry and Urinalysis*

Clinical biochemical parameters associated with renal injury including serum total protein, serum creatinine, and BUN were assessed (7170 automated analyzer; Hitachi, Tokyo, Japan). Urinalysis parameters measured included urinary total protein and urinary creatinine levels (Fuji Dri-Chem FDC7000; Fuji Film, Tokyo, Japan). All procedures were performed according to the manufacturers' protocols.

*Renal Histopathology and Immunohistochemistry*

The fixed kidneys were dehydrated, embedded in paraffin, cut into approximately 3-μm thick sections. To evaluate glomerular region, sections were stained with hematoxylin and eosin (HE) and periodic acid-Schiff (PAS). The degree of histopathological change was determined and scored on a scale of 0–4 as follows: 0 = no findings, 1 = slight changes, 2 = mild changes, 3 = moderate changes, and 4 = severe changes. To analyze deposition of antibodies, immunohistochemical staining for immunoglobulin (Ig) A, IgG and IgM were also conducted. Sections were treated with protease K (Dako, Glostrup, Denmark) for 10 min for antigen retrieval, and then incubated with primary antibody for 1 h at room temperature. After washing with Tris-buffered saline with Tween-20 (pH 7.6), the sections were incubated with secondary antibody for 1 h at room temperature. The primary antibodies were polyclonal goat anti-mouse IgA (code No. A90-103P; Bethyl Laboratories, Montgomery, Tex., USA), goat anti-mouse IgG (code No. 710-1332; Rockland Immunochemicals, Gilbertsville, Pa., USA) and goat anti-mouse IgM (code No. A90-101P; Bethyl Laboratories) and used at dilution of 1:100. The second antibody was Alexa Fluor 488-labeled chicken anti-goat IgG antibody (code No. A-21467; Molecular Probes, Eugene, Oreg., USA) and used at dilution of 1:200. The sections were visualized with fluorescence microscopy (DMRBE; Leica Microsystems, GmbH, Wetzlar, Germany). Images were ex-

**Table 1.** Blood chemistry and urinalysis

| | 4 weeks | | 8 weeks | |
|---|---|---|---|---|
| | ICR (4) | ICGN (8) | ICR (4) | ICGN (10) |
| BUN, mg/dl | 19.5±1.9 | 34.0±6.7** | 24.5±3.1 | 31.9±10.6 |
| Serum creatinine, mg/dl | 0.10±0.00 | 0.10±0.00 | 0.05±0.06 | 0.16±0.16 |
| Serum total protein, g/dl | 4.05±0.19 | 3.90±0.30 | 4.95±0.31 | 2.89±0.49** |
| Urinary total protein, g/dl | 0.25±0.10 | 0.41±0.32 | 1.50±0.36 | 3.05±0.98* |
| Urinary creatinine, mg/dl | 152.5±17.1 | 65.6±17.3** | 312.5±110.9 | 48.6±20.4** |

Data represent mean ± SD. * $p < 0.05$ and ** $p < 0.01$ compared with age-matched ICR mice. The number of mice examined is shown in parentheses.

ported from the Pixcera digital camera system (Penguin 600CL/In Studio v.1.0; Pixcera Corp., Los Gatos, Calif., USA).

*Microarray Analysis*

Microarray analysis was conducted with RNA harvested from the renal cortex of 4- and 8-week-old ICGN and ICR mice. The samples of renal cortex were separated from the slices fixed in RNA*later*® as previously reported [12] and homogenized using the Mill Mixer (Qiagen, Hilden, Germany) with zirconium beads. Total RNA was isolated from the kidney homogenate using the RNeasy kit (Qiagen). Microarray analysis was conducted by using the GeneChip® Mouse Genome 430 2.0 Array (Affymetrix, Santa Clara, Calif., USA). The procedure was conducted according to the manufacturer's instructions. cDNA synthesis and purification were performed with the Superscript Choice System (Invitrogen), the T7-(dT)24-oligonucleotide primer (Affymetrix), and the cDNA Cleanup Module (Affymetrix). The biotinylated cRNA synthesis and purification were performed using the GeneChip Expression 3-Amplification Reagents for IVT Labeling (Affymetrix) and the cRNA Cleanup Module (Affymetrix). Fragmented cRNA (20 μg) was hybridized to a Mouse Genome 430 2.0 Array for 18 h at 45°C at 60 rpm, after which the array was washed and stained by streptavidin-phycoerythrin (Fluidics Station 400; Affymetrix) then scanned by the Gene Array Scanner (Affymetrix). Non-normalized MAS5 signals were imported into the Microsoft Office Excel 2007 (Microsoft Corp., Redmond, Wash., USA) and normalized for each microarray by setting the mean signal intensity to be equal across microarrays. The normalized ICGN values were compared to age-matched ICR values and expressed as fold change (ICGN/ICR). The Student's t test p values were calculated using the Microsoft Office Excel 2007. The data discussed in this publication have been deposited in NCBI's Gene Expression Omnibus and are accessible through GEO Series accession No. GSE 45005 (http://www.ncbi.nlm.nih.gov/geo/query/acc.cgi?acc=GSE45005).

*Pathway Analysis*

Genes for the canonical pathway analysis were selected using the fold change cutoff of >2 or <-2 and the p value cutoff of <0.01. Pathway analysis was conducted using the Ingenuity Pathway Analysis software (IPA; Ingenuity Systems, Redwood City, Calif., USA; www.ingenuity.com). This software identified the canonical pathways from the IPA library of canonical pathways that were most significant to the selected genes. Fisher's exact test was used to calculate a p value determining the probability that the association between the genes in the dataset and the canonical pathway was due to chance.

*Quantitative PCR*

Single-stranded cDNA was synthesized from 1 μg of total liver RNA using the High Capacity RNA-to-cDNA Master Mix (Applied Biosystems, Foster City, Calif., USA). Quantitative PCR was performed on the ABI Prism 7900 (Applied Biosystems), using the TaqMan Universal Master Mix II (Applied Biosystems) with sets of primers and Universal ProbeLibrary probes (Roche, Basel, Switzerland) designed online with the ProbeFinder version 2.45 for mouse (Roche). Probes specific for mouse *C1s* (forward primer: 5′-TGGATACTTCTGCTCCTGTCC, reverse primer: 5′-CAGGGCAGTGAACACATCTC, and Universal ProbeLibrary probe #69, which gives a 94-nt amplicon); and β-actin (Actb) (forward primer: 5′-CTAAGGCCAACCGTGAAAAG, reverse primer: 5′-ACCAGAGGCATACAGGGACA, and Universal ProbeLibrary probe #64, which gives a 104-nt amplicon) were used. Each sample was amplified with 1 cycle at 95°C for 10 min (to activate the polymerase) and followed by 40 cycles at (95°C for 15 s and 60°C for 1 min).

*ELISA of Anti-Double-Stranded DNA Antibody*

Serum anti-double-stranded (ds)DNA antibody was measured using a mouse anti-dsDNA ELISA Kit (Shibayagi, Gunma, Japan) according to the manufacturer's instructions.

*Statistical Analysis*

Aspin-Welch's t test was performed for ELISA of anti-dsDNA antibody. Student's t test was performed for all other measured values. For the microarray data, p values <0.01 were considered significant while for all other data, p values <0.05 were considered significant.

## Results

### *Clinical Biochemistry and Urinalysis*

Blood and urinary biochemical parameters are summarized in table 1. At 4 weeks of age, ICGN mice showed

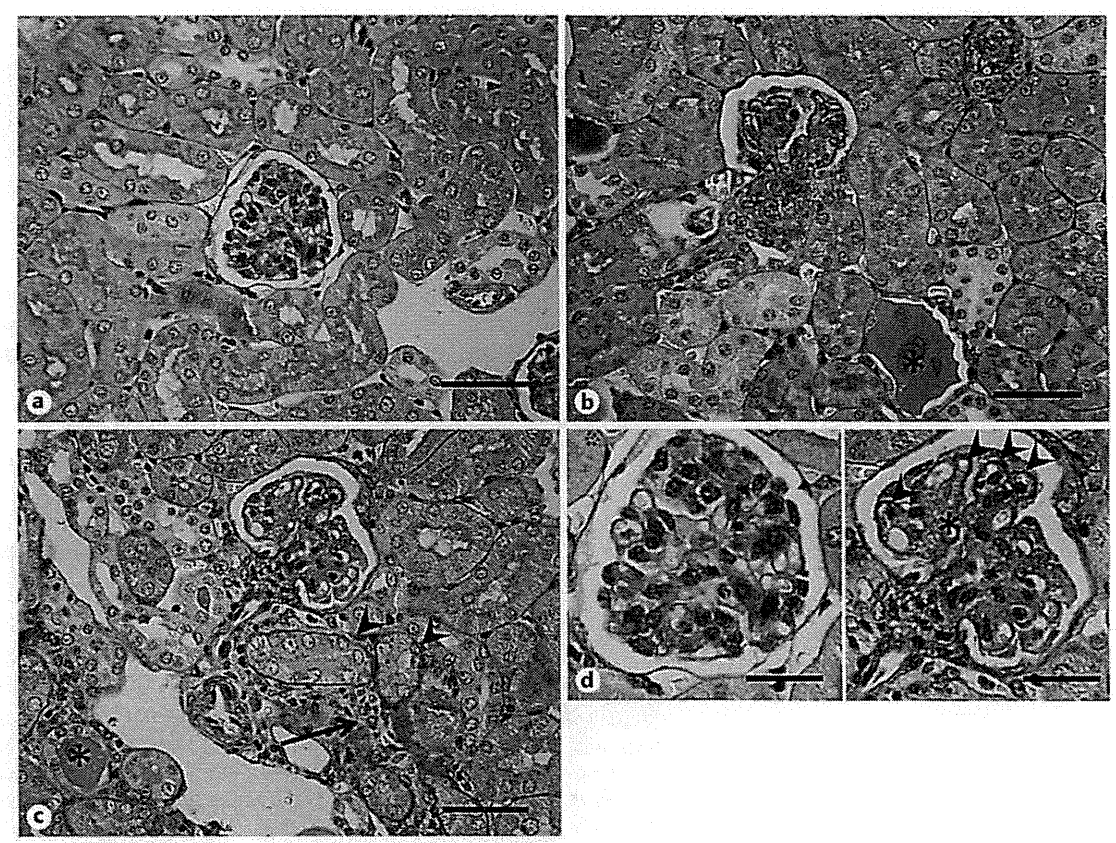

**Fig. 1.** Kidney sections from 4-week-old ICR (**a**), 4-week-old ICGN (**b**) and 8-week-old ICGN (**c**) mice were stained with PAS. High magnifications of glomerulus in 4-week-old ICR (left) and 8-week-old ICGN (right) mice are shown (**d**). Glomeruli with expanded mesangial area/thickening of the GBM and protein cast (asterisk) were observed in 4-week-old ICGN mice (**b**). In 8-week-old ICGN mice (**c**), not only lesions found in 4-week-old ICGN mice had progressed but inflammatory cell infiltration (arrows) and basophilic tubules (arrowheads) had become marked. Glomeruli in 8-week-old ICGN mice showed prominent mesangial area expansion (asterisk) and thickening of the GBM (arrowheads) (**d**). Bars: **a–c** 50 μm; **d** 25 μm.

**Table 2.** Histopathological examination of ICR and ICGN mouse kidney

| Findings | Grade[a] | 4 weeks | | 8 weeks | |
|---|---|---|---|---|---|
| | | ICR (4) | ICGN (8) | ICR (4) | ICGN (10) |
| Expansion of mesangial areas/ thickening of the GBM | 0 | 4 | 0 | 4 | 0 |
| | 1 | 0 | 7 | 0 | 0 |
| | 2 | 0 | 1 | 0 | 4 |
| | 3 | 0 | 0 | 0 | 6 |
| | 4 | 0 | 0 | 0 | 0 |
| Tubulointerstitial injury | 0 | 4 | 4 | 4 | 0 |
| | 1 | 0 | 4 | 0 | 1 |
| | 2 | 0 | 0 | 0 | 4 |
| | 3 | 0 | 0 | 0 | 3 |
| | 4 | 0 | 0 | 0 | 2 |

The number of mice examined is shown in parentheses.
[a] Grade of change: 0 = negative, 1 = slight, 2 = mild, 3 = moderate, 4 = severe.

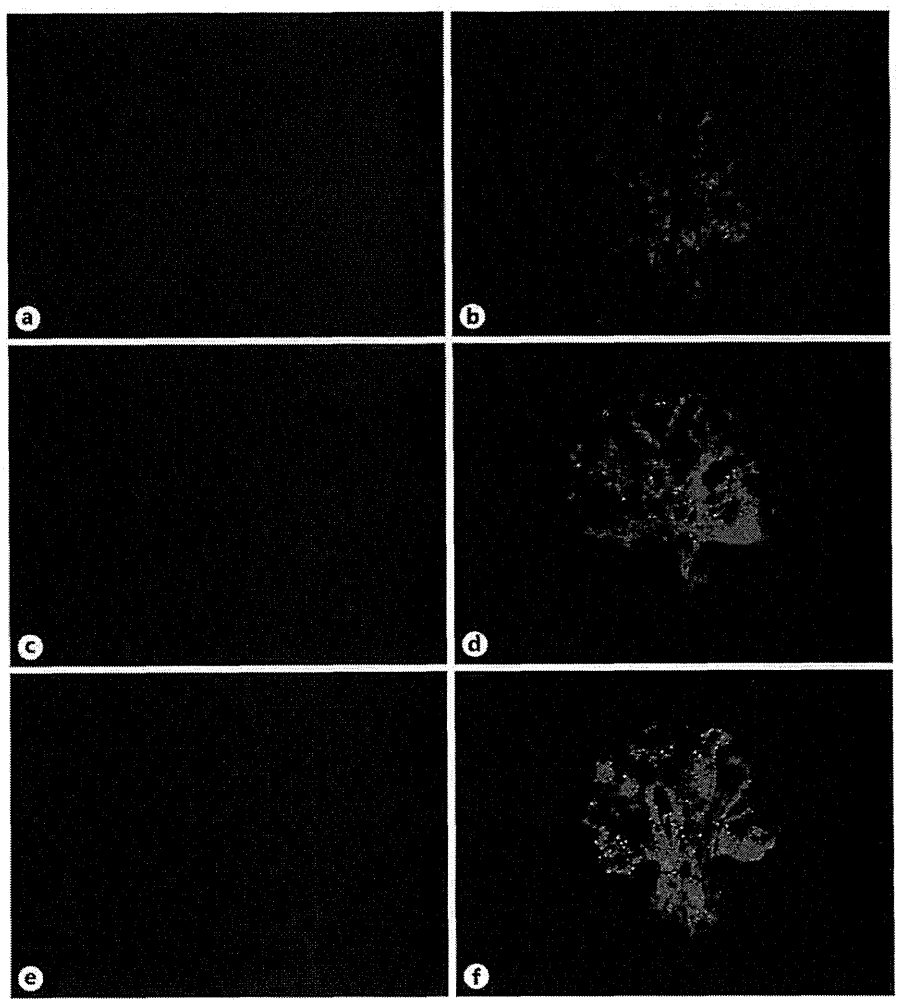


**Fig. 2.** Representative photographs of IgA, IgG and IgM immunostaining. Kidney sections of 8-week-old ICR (**a**, **c**, **e**) and ICGN (**b**, **d**, **f**) mice were stained with antibodies to IgA (**a**, **b**), IgG (**c**, **d**) and IgM (**e**, **f**). Positive reactions were observed in GBM of ICGN mice (**b**, **d**, **f**).

significant increase in BUN (1.74-fold higher than the ICR control values) and significant decrease in urinary creatinine levels (43% of the ICR control values). At 8 weeks of age, ICGN mice showed markedly lower urinary creatinine levels (15.6% of ICR control levels), hypoproteinemia (58.4% of the ICR control values) and proteinuria (2.03-fold higher than the ICR control values).

*Renal Histopathology and Immunohistochemistry*

Histopathological examination is summarized in table 2. All 4-week-old ICGN mice exhibited slight to mild mesangial expansion and thickening of the GBM and by 8 weeks of age, all the mice showed mild to moderate GBM findings (table 2; fig. 1d). In addition, 4 of 8 ICGN mice examined at 4 weeks of age showed slight tubulointerstitial injury consisting of inflammatory cell infiltration, basophilic tubules and protein cast (table 2; fig. 1b). By 8 weeks of age, all of the ICGN mice showed slight to severe tubulointerstitial findings (table 2; fig. 1c). Immunohistochemical analysis revealed depositions of IgA, IgG and IgM on the thickened GBM of 4- and 8-week-old ICGN mice (fig. 2).

*Microarray Analysis*

A total of 252 and 807 transcripts met the filtering criteria (fold change value of >2 or <-2 and p value of <0.01) in the renal cortical tissue of 4- and 8-week-old ICGN mice, respectively. Of these, a total of 37 transcripts overlapped at the 4- and 8-week time period. A list of the 37 overlapping transcripts are presented in table 3 and are arranged in order of absolute value of fold change at 4 weeks of age (early stage of nephrotic syndrome). Of these 37 genes, *C1s* gene showed the largest change (2.2% of ICR control levels at 4 weeks of age).

**Table 3.** List of differentially regulated genes in ICGN mouse kidney at both of 4 and 8 weeks of age

| Probe set ID | Gene symbol | Entrez gene name | Fold change | |
|---|---|---|---|---|
| | | | 4 weeks | 8 weeks |
| 1424041_s_at | *C1s* | Complement component 1, s subcomponent | −45.1 | −26.8 |
| 1423487_at | *Cript* | Cysteine-rich PDZ-binding protein | −16.0 | −5.4 |
| 1418837_at | *Qprt* | Quinolinate phosphoribosyltransferase | 6.1 | 6.1 |
| 1438858_x_at | *H2-Aa* | Histocompatibility 2, class II antigen A, α | 5.1 | 5.5 |
| 1449526_a_at | *Gdpd3* | Glycerophosphodiester phosphodiesterase domain containing 3 | 4.8 | 31.7 |
| 1422141_s_at | *Csprs* | Component of Sp100-rs | 4.7 | 7.2 |
| 1460416_s_at | *Csprs /// Gm7592 /// Gm7609 /// LOC100503923* | Component of Sp100-rs /// predicted gene 7592 /// predicted pseudogene 7609 /// hypothetical protein LOC100503923 | 4.2 | 4.4 |
| 1434833_at | *Map4k2* | Mitogen-activated protein kinase kinase kinase kinase 2 | −4.0 | −3.8 |
| 1452264_at | *Tenc1, Tns2* | Tensin-like C1 domain-containing phosphatase (tensin 2) | −4.0 | −3.4 |
| 1424727_at | *Ccr5* | Chemokine (C-C motif) receptor 5 | 3.9 | 3.4 |
| 1445293_at | – | – | −3.4 | −4.3 |
| 1426324_at | *H2-D1* | Histocompatibility 2, D region locus 1 | 3.2 | 3.2 |
| 1421211_a_at | *Ciita* | Class II transactivator | 3.1 | 8.1 |
| 1425951_a_at | *Clec4n* | C-type lectin domain family 4, member n | 3.1 | 3.7 |
| 1448734_at | *Cp* | Ceruloplasmin | 2.9 | 15.3 |
| 1417495_x_at | *Cp* | Ceruloplasmin | 2.9 | 14.4 |
| 1452661_at | *Tfrc* | Transferrin receptor | −2.8 | −2.5 |
| 1436905_x_at | *Laptm5* | Lysosomal-associated protein transmembrane 5 | 2.7 | 4.6 |
| 1441975_at | *Acpp* | Acid phosphatase, prostate | 2.6 | 2.9 |
| 1437217_at | *Ankrd6* | Ankyrin repeat domain 6 | 2.6 | 3.9 |
| 1442436_at | *Fn3k* | Fructosamine 3 kinase | −2.6 | −2.1 |
| 1457753_at | *Tlr13* | Toll-like receptor 13 | 2.5 | 2.9 |
| 1448591_at | *Ctss* | Cathepsin S | 2.5 | 5.7 |
| 1416318_at | *Serpinb1a* | Serine (or cysteine) peptidase inhibitor, clade B, member 1a | 2.4 | 2.6 |
| 1426601_at | *Slc37a1* | Solute carrier family 37 (glycerol-3-phosphate transporter), member 1 | 2.4 | 3.8 |
| 1436778_at | *Cybb* | Cytochrome b-245, β polypeptide | 2.3 | 3.6 |
| 1435906_x_at | *Gbp2* | Guanylate binding protein 2 | 2.3 | 3.5 |
| 1424942_a_at | *Myc* | Myelocytomatosis oncogene | 2.3 | 3.2 |
| 1418674_at | *Osmr* | Oncostatin M receptor | 2.2 | 2.9 |
| 1455700_at | *Mterfd3* | MTERF domain containing 3 | 2.2 | 2.2 |
| 1433699_at | *Tnfaip3* | Tumor necrosis factor-α-induced protein 3 | 2.1 | 4.4 |
| 1448748_at | *Plek* | Pleckstrin | 2.1 | 3.2 |
| 1415698_at | *Golm1* | Golgi membrane protein 1 | 2.1 | 3.6 |
| 1419004_s_at | *Bcl2a1a ///Bcl2a1b /// Bcl2a1d* | B cell leukemia/lymphoma 2-related protein A1a /// B cell leukemia/lymphoma 2-related protein A1b /// B cell leukemia/lymphoma 2-related protein A1d | 2.1 | 4.5 |
| 1460259_s_at | *Clca1 /// Clca2* | Chloride channel calcium activated 1 /// chloride channel calcium activated 2 | 2.1 | 3.4 |
| 1417852_x_at | *Clca1* | Chloride channel calcium activated 1 | 2.0 | 2.7 |
| 1450869_at | *Fgf1* | Fibroblast growth factor 1 | −2.0 | −2.4 |

Data represent fold change value (ICGN/ICR, n = 3).

**Table 4.** Canonical pathways affected significantly in ICGN mouse kidney as compared with ICR mice kidney

| Canonical pathway | Signaling pathway categories | -log (p value) | |
|---|---|---|---|
| | | 4 weeks | 8 weeks |
| Type 1 diabetes mellitus signaling | Apoptosis; disease-specific pathways | 5.26 | |
| Role of NFAT in regulation of the immune response | **Cellular immune response; humoral immune response;** intracellular and second messenger signaling | 4.33 | |
| Acute phase response signaling | **Cytokine signaling;** ingenuity toxicity list pathways | 4.2 | |
| NF-κB activation by viruses | **Cellular immune response;** pathogen-influenced signaling | 3.79 | |
| PKCθ signaling in T lymphocytes | **Cellular immune response** | 3.49 | |
| Virus entry via endocytic pathways | Pathogen-influenced signaling | 3.34 | |
| Nur77 signaling in T lymphocytes | Apoptosis; **cellular immune response;** nuclear receptor signaling | 3.07 | |
| Systemic lupus erythematosus signaling | Disease-specific pathways | 3.02 | |
| Calcium-induced T-lymphocyte apoptosis | Apoptosis; **cellular immune response** | 2.75 | |
| CD28 signaling in T-helper cells | **Cellular immune response** | 2.75 | |
| CTLA4 signaling in cytotoxic T lymphocytes | **Cellular immune response** | 2.64 | |
| IL-6 signaling | **Cellular immune response; cytokine signaling** | 2.61 | |
| Docosahexaenoic acid (DHA) signaling | Intracellular and second messenger signaling; neurotransmitters and other nervous system signaling | 2.53 | |
| IL-4 signaling | **Cellular immune response; cytokine signaling; humoral immune response** | 2.45 | |
| iCOS-iCOSL signaling in T-helper cells | **Cellular immune response** | 2.3 | |
| Rac signaling | Intracellular and second messenger signaling | 2.26 | |
| TNFR1 signaling | Apoptosis; **cytokine signaling** | 2.22 | |
| fMLP signaling in neutrophils | **Cellular immune response; cytokine signaling** | 2.22 | |
| Graft-versus-host disease signaling | **Cellular immune response;** disease-specific pathways | 5.74 | 5.38 |
| Antigen presentation pathway | **Cellular immune response; humoral immune response** | 5.42 | 4.95 |
| Autoimmune thyroid disease signaling | **Cellular immune response;** disease-specific pathways; **humoral immune response** | 4.8 | 4.06 |
| Complement system | **Humoral immune response** | 4.36 | 3.43 |
| Allograft rejection signaling | **Cellular immune response;** disease-specific pathways | 4.32 | 3.39 |
| Dendritic cell maturation | **Cellular immune response; cytokine signaling;** pathogen-influenced signaling | 4.27 | 5.92 |
| IL-10 signaling | **Cellular immune response; cytokine signaling** | 4.03 | 2.94 |
| Role of pattern recognition receptors in recognition of bacteria and viruses | **Cellular immune response;** pathogen-influenced signaling | 3.98 | 3.27 |
| OX40 signaling pathway | **Cellular immune response** | 3.82 | 2.73 |
| Altered T cell and B cell signaling in rheumatoid arthritis | **Cellular immune response;** disease-specific pathways | 3.64 | 7.49 |
| B cell development | Cellular growth, proliferation and development; **humoral immune response** | 3.25 | 5.44 |
| Communication between innate and adaptive immune cells | **Cellular immune response** | 3.16 | 7.77 |
| Cytotoxic T-lymphocyte-mediated apoptosis of target cells | Apoptosis; **cellular immune response** | 3.15 | 3.15 |
| Crosstalk between dendritic cells and natural killer cells | **Cellular immune response** | 3.02 | 2.22 |
| Hepatic fibrosis/hepatic stellate cell activation | Disease-specific pathways; ingenuity toxicity list pathways | 2.83 | 6.97 |
| Pathogenesis of multiple sclerosis | Disease-specific pathways | 2.16 | 4.54 |
| TREM1 signaling | **Cellular immune response; cytokine signaling** | 2.12 | 2.27 |
| Role of hypercytokinemia/hyperchemokinemia in the pathogenesis of influenza | **Cellular immune response; cytokine signaling** | 2.03 | 4.04 |
| LXR/RXR activation | Ingenuity toxicity list pathways; nuclear receptor signaling | 2.02 | 3.27 |
| Atherosclerosis signaling | Cardiovascular signaling; disease-specific pathways | | 4.39 |
| Intrinsic prothrombin activation pathway | Cardiovascular signaling; cellular stress and injury | | 3.32 |
| T-helper cell differentiation | **Cellular immune response; cytokine signaling** | | 2.66 |
| Primary immunodeficiency signaling | **Cellular immune response;** disease-specific pathways; **humoral immune response** | | 2.29 |

Bold font: significantly affected pathways which were categorized into 'Humoral immune response', 'Cellular immune response' and/or 'Cytokine signaling'.